

A Synopsis of the Thesis Entitled

Processing and Characterization of In-Situ Aluminium Matrix Composite by Stir Casting Method

is submitted to

THE MAHARAJA SAYAJIRAO UNIVERSITY OF BARODA

in the partial fulfillment of the requirements for the degree of

Doctor of Philosophy

in

METALLURGICAL AND MATERIALS ENGINEERING

by

Hemantkumar Narendrabhai Panchal

Research Guide

Dr. Vandana J. Rao



Metallurgical and Materials Engineering Department

Faculty of Technology and Engineering

The Maharaja Sayajirao University of Baroda

Vadodara – 390001, Gujarat (India)

2020-2021

Table of Contents

Table of Content.....	2
1. INTRODUCTION	3
1.1 Aluminium Composite Materials.....	3
1.2 Present Work	3
2. EXPERIMENTAL WORK	4
2.1 Phase I: Optimization of magnesium content into the commercially pure aluminium (CPA)	6
2.2 Phase II: Effect of variation of MnO ₂ by changing its addition sequence in CPA	6
2.3 Phase III: Effect of variation of MnO ₂ by changing its addition sequence in CPA along with optimized magnesium metal from phase I study	7
3. RESULTS AND DISCUSSION:.....	9
3.1 Raw Materials	9
3.2 Phase I: Optimization of magnesium content into the commercially pure aluminium (CPA) ...	10
3.2.1 Chemical analysis.....	10
3.2.2 XRD Analysis	10
3.2.3 Density and ductility.....	11
3.2.4 Strength and hardness	11
3.2.5 Microstructure.....	11
3.3 Phase II: Effect of variation of MnO ₂ by changing its addition sequence in CPA	15
3.3.1 Chemical analysis.....	15
3.3.2 X-Ray Diffraction.....	16
3.3.3 Density and ductility.....	16
3.3.4 Strength and hardness	17
3.3.5 Microstructure.....	17
3.4 Phase III: Effect of variation of MnO ₂ by changing its addition sequence in CPA along with optimized magnesium metal from phase I study	19
3.4.1 Chemical analysis.....	19
3.4.2 X-Ray Diffraction	20
3.4.3 Density and ductility.....	21
3.4.4 Strength and hardness	22
3.4.5 Microstructure.....	22
4. CONCLUSION.....	24
REFERENCES.....	26

1. INTRODUCTION

1.1 Aluminium Composite Materials

Aluminium and its alloys are commonly used in variety of application in different sectors such as aerospace, automobile, defence, domestic purpose, etc. since past many years. It also found many advance applications due to some of the excellent properties at low cost. Major properties which are concerned in aluminium and its alloys are strength, density, durability, machinability, etc.

There are different processing methods to fabricate the metal matrix composites. Based on the addition of reinforcement material to the matrix there are two different processing techniques like *ex-situ* and *in-situ*. In *ex-situ* process, the metal matrix composite is developed by adding the reinforcement directly to the molten matrix material. The reinforcement is developed within the matrix by adding various ceramic particles such as oxides, carbides, nitrides or even halide salts to the molten matrix material. The reinforcement is developed by the exothermic reaction between the elements or their compounds with molten aluminium alloy. *In-situ* technique is suitable to produce new composite materials that are not obtained by conventional methods. The *in-situ* process is having several advantages like uniform distribution of reinforcement, development of fine reinforcement particles and fine interface between the matrix and reinforcement. Synthesis of MMCs by casting is the economical processing route to develop *in-situ* metal matrix composites with the uniform distribution of the reinforcement.

Aluminium Matrix Composites (AMCs) can be classified into *four* types depending on the type of reinforcement added into the matrix like:

- a) Particle-reinforced AMCs (PAMCs)
- b) Whisker-or short fibre-reinforced AMCs (SFAMCs)
- c) Continuous fibre-reinforced AMCs (CFAMCs)
- d) Mono filament-reinforced AMCs (MFAMCs)

1.2 Present Work

The main aim of present research work is to improve the properties of commercially pure aluminium (CPA) by varying different parameters like amount of particulate reinforcement and its sequence of addition. Selected reinforcement is MnO_2 because it is stable up to the temperature at around 500°C , above which decomposition take place ^[1] at 535°C and generates oxide particles. Optimization of magnesium was also checked for proper wetting of generated oxides or any other phases. The process parameters are reported in Table 1. To check the effects of additions, detail analysis has been carried out in three different phases of experiments:

- Phase I** : Optimization of magnesium content into the commercially pure aluminium (CPA)
Phase II : Effect of variation of MnO_2 content by changing its addition sequence in CPA and
Phase III : Effect of variation of MnO_2 by changing its addition sequence in CPA along with optimized magnesium metal from phase I study.

Followings are the objectives of the research work:

1. To optimise the amount of wetting agent for commercially pure aluminium,
2. To study the variation of reinforcement and its sequence of addition,
3. To study generated in-situ phases after optimised the wetting agent and reinforcement oxides,
4. To study the microstructure and mechanical properties of generated in-situ composite material and
5. To compare the properties of existing material with new in-situ route.

Table 1: Parameters and properties studied

Sr. No.		Description
1	Parameters	Amount of reinforcement, Sequence of reinforcement addition,
2	Properties	Chemical analysis (spectroscopy) XRD Density, Ductility, Hardness, Tensile strength and Microstructure.

2. EXPERIMENTAL WORK

In present work, melting and casting route was followed for fabrication of aluminium matrix composite with MnO₂ reinforcement. Following is the summarised flow chart of the experimental work presented in figure 1.

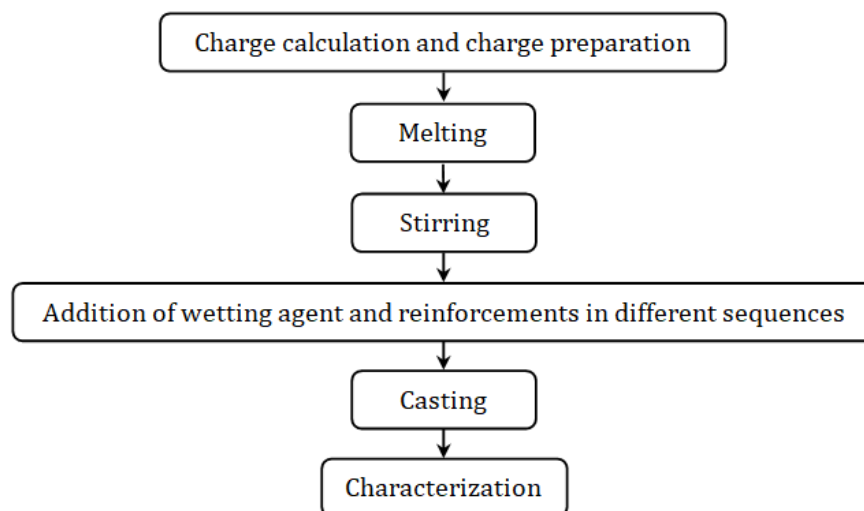


Figure 1: Generalised flow sheet of present work methodology.

Following figure 2 shows the experimental set up used in this research work.

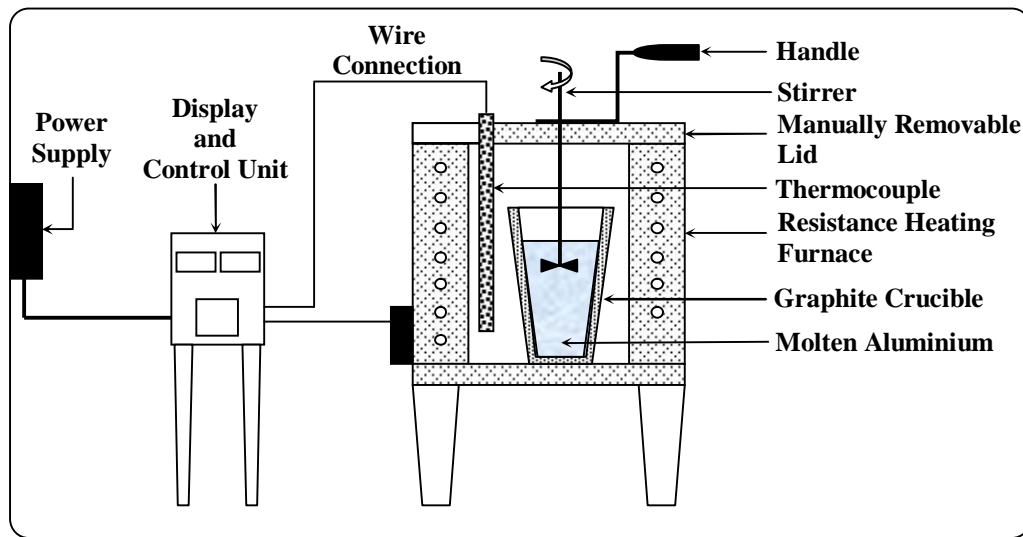


Figure 2 Experimental set up

List of different process parameters are mentioned in table 2.

Table 2 Process Parameters

Sr. No.	Process Parameter	Process Variables		
		Phase I	Phase II	Phase III
1	Amount of Commercially Pure Al	700 gm	700 gm	700 gm
2	Processing temperature	720 °C	720 °C	720 °C
3	Time of processing	15 min	15 min	15 min
4	Stirrer speed	100 RPM	100 RPM	100 RPM
5	Amount of Commercially Pure Magnesium addition	0.05, 0.15, 0.5, 1, 1.5, 2, 3, 4, 5, 6 and 7*	--	3*
6	Amount of MnO ₂ addition	--	0.5, 1, 1.5, 2, 2.5, 3, 3.5 and 4*	1, 2.5 and 4*
7	Sequence of MnO ₂ addition	--	A and B [#]	A and B [#]

*All compositions are in weight percent unless stated otherwise

[#]Sequence A: MnO₂ added after melting of commercially pure aluminium and Sequence B: MnO₂ added before melting of commercially pure aluminium

2.1 Phase I: Optimization of magnesium content into the commercially pure aluminium (CPA)

Phase I study involved the addition of commercially pure magnesium into commercially pure aluminium. As shown in table 2 of process parameters, there were 11 runs of experiments carried out to check the effect of magnesium along with one run without Mg addition.

Experimental steps in the form of flow-sheet are shown in figure 3 below. It indicates the detailed procedure of the experimentations followed during phase I. These experiments are to determine the optimum level of magnesium for present CPA. As received compositions of CPA and magnesium is already discussed in table 3.

As shown in table 2, process parameters are used. 720 °C temperature and 15 minutes time were kept fixed for all the experiments for 700 gm charge materials. Magnesium amount was varied from 0.05 to 7 wt %.

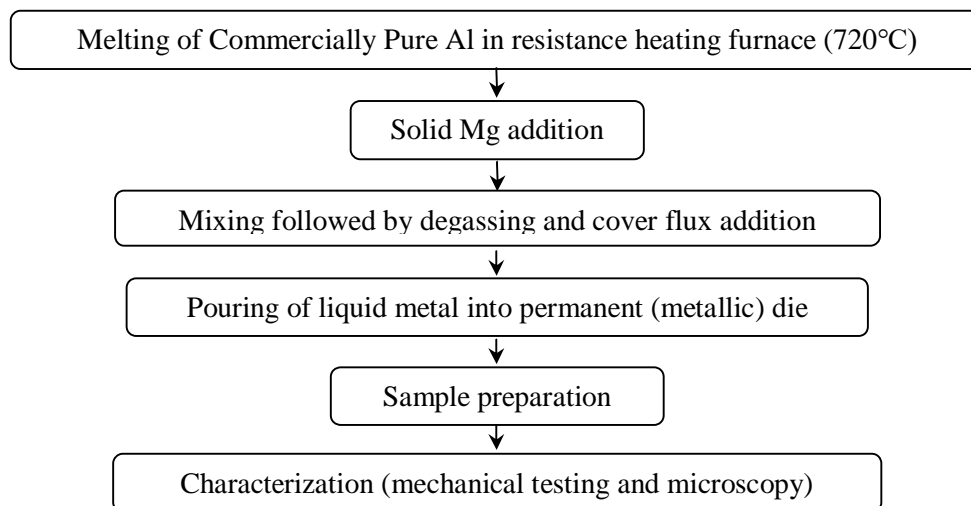


Figure 3 Flow sheet of experimental steps followed in phase I.

SiC rod is used to dip the lighter magnesium solid piece until it melts into the bath. Mechanical stirring was carried out at constant 100 RPM speed for agitating the bath for required time periods till uniform mixture was achieved. This was followed by standard melting practice to remove the dissolved gases followed by liquid metal pouring into permanent die.

2.2 Phase II: Effect of variation of MnO₂ by changing its addition sequence in CPA

Phase II study involved the addition of MnO₂ into commercially pure aluminium (CPA) without addition of commercially pure magnesium. As shown in table 2 of process parameters, there were 16 runs of experiments carried out to check the effect of MnO₂ by changing the sequence of addition. 0.5, 1, 1.5, 2, 2.5, 3, 3.5 and 4 wt % MnO₂ in two different sequences (A and B) have been added into Al to check its effect on properties and microstructures. Below flow-sheets explain experimentations for phase II.

Sequence A: MnO₂ addition in commercially pure aluminium **after** melting.

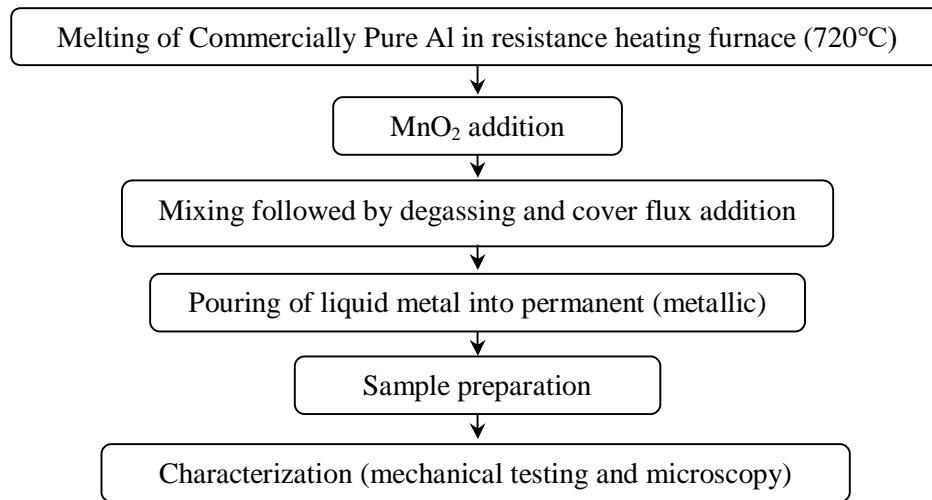


Figure 4 Flow sheet of experimental steps followed in sequence A of phase II.

Sequence B: MnO₂ addition in commercially pure aluminium **before** melting.

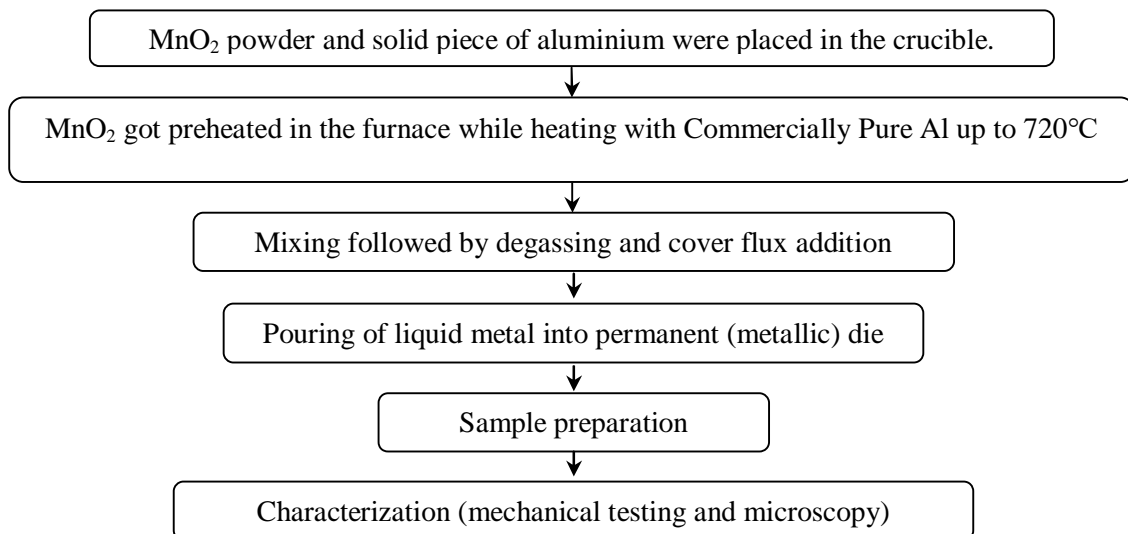


Figure 5 Flow-sheet of experimental steps followed in sequence B of phase II.

2.3 Phase III: Effect of variation of MnO₂ by changing its addition sequence in CPA along with optimized magnesium metal from phase I study

Phase III study involved the addition of Mg and MnO₂ both into commercially pure aluminium in two different sequences (A and B as mentioned in table 2). There were total 06 runs of experiments, three in each sequence, carried out to check the effect of magnesium and MnO₂ by changing its sequence of addition on various properties on CPA matrix. From phase-I results, optimum value of magnesium in

commercially pure aluminium was 3 wt%. Hence, keeping this result in mind, we have fixed the magnesium content at 3 wt%, whereas MnO_2 concentration was varied as 0.5, 2.5 and 4 wt % in two different sequences (A and B). As mentioned below flow-sheet, experimentations have been followed.

Sequence A: MnO_2 addition in commercially pure aluminium **after** melting

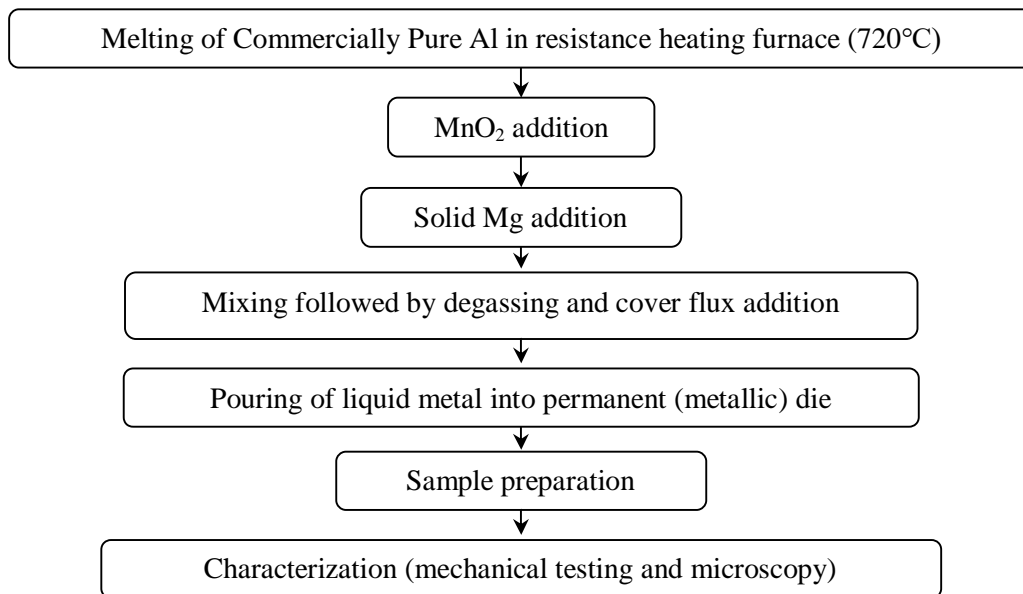


Figure 6 Flow sheet of experimental steps followed in sequence A of phase III.

Sequence B: MnO_2 addition in commercially pure aluminium **before** melting

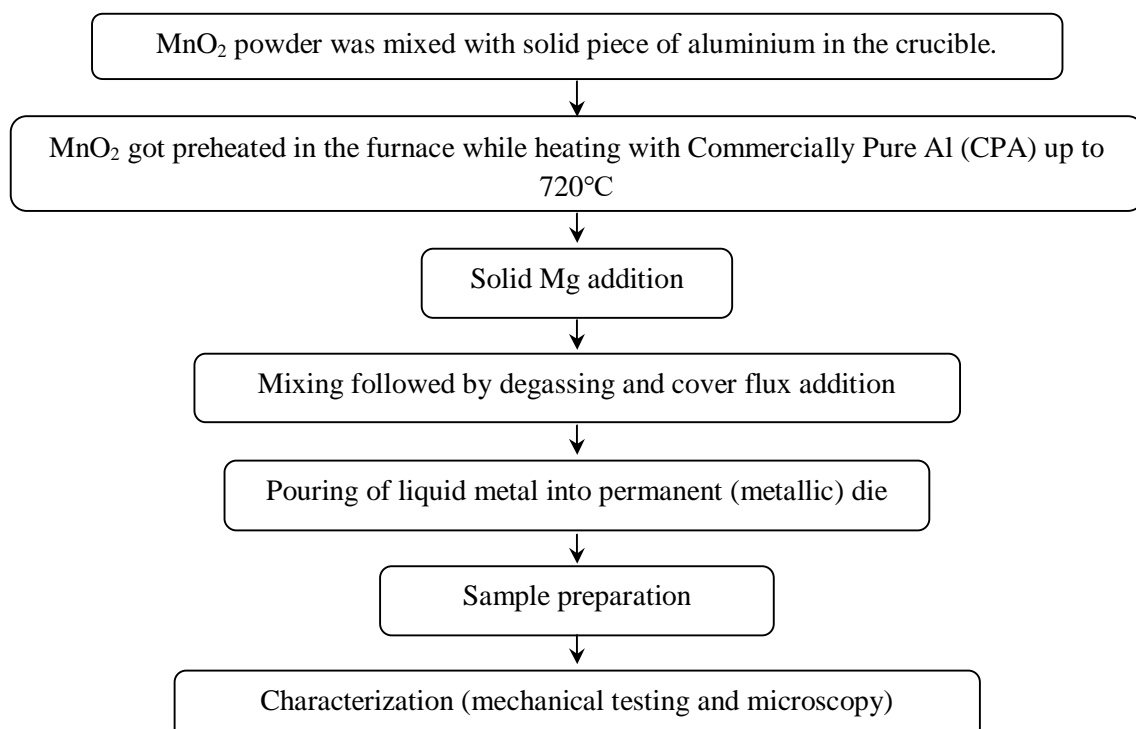


Figure 7 Flow sheet of experimental steps followed in sequence B of phase III.

3. RESULTS AND DISCUSSION:

3.1 Raw Materials

Chemical compositions of *raw materials* in as received condition are as shown in table 3. The XRD Pattern of as received commercially pure (CP) aluminium and MnO₂ is given in figure 8 whereas figure 2.2 represents the schematic diagram of the experiment set-up used.

Table 3 Chemical compositions of commercially pure (CP) aluminium, Magnesium and MnO₂ in as received condition.

Materials	Element Composition (wt %)										
	Si	Mn	Mg	Fe	Cu	Zn	C	O	K	Al	Total
CP Aluminium	0.05	0.02	0.03	0.42	0.05	0.04	--	--	--	99.39	100
Magnesium	0.13	--	99.68	--	--	--	--	--	--	0.19	100
MnO ₂	0.81	51.61	--	3.09	--	--	7.6	35.56	0.82	0.51	100

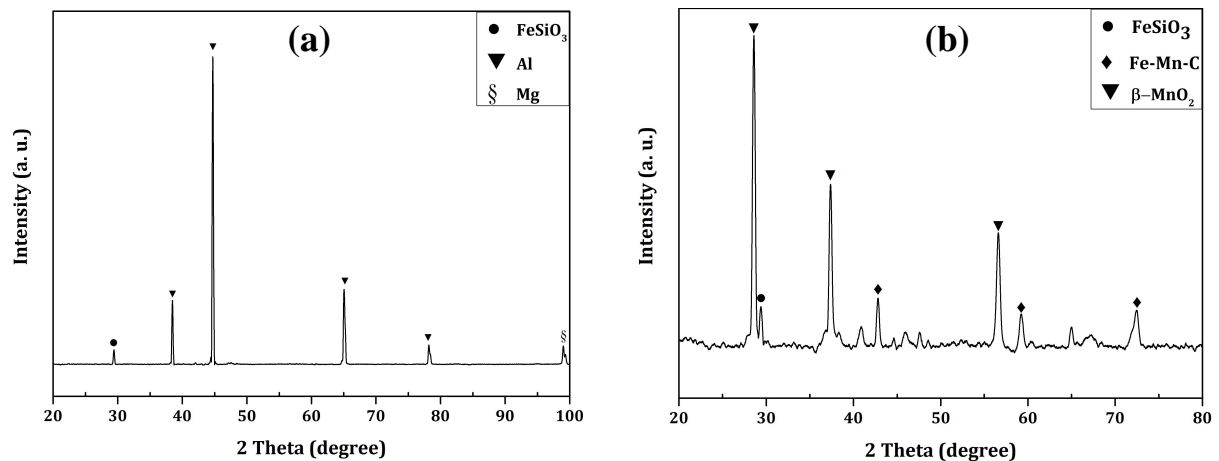


Figure 8 Typical XRD pattern of raw (a) commercially pure aluminium and (b) MnO₂ powder.

Sieve analysis of raw MnO₂ powder has been performed to check the size distribution. We observed that the size of MnO₂ powder used in this work was 75 to 44 micron and less as shown in following table.

Table 4 Sieve analysis of MnO₂ powder.

Sr. No.	BSS Mesh Number	Size (micron)	Content (wt %)
1	-60 +100	150	0.143
2	-100 +120	125	0.291
3	-120 +150	100	0.073
4	-150 +200	75	13.326
5	-200 +300	53	23.259
6	-300 +350	44	17.902
7	PAN	--	41.916

3.2 Phase I: Optimization of magnesium content into the commercially pure aluminium (CPA)

3.2.1 Chemical analysis

Table 5 shows spectroscopy results of different experiments of Al-Mg system.

Table 5 Chemical compositions of various Al-Mg systems by spectroscopy (Element Recovery)

Experiments	wt % Mg added	Element Composition (wt %)						
		O	Mg	Si	Mn	Fe	Al	Total
1	0.00	14.2	0.05	0.27	0.015	0.37	85.095	100
2	0.05	11.2	0.04	0.15	0.017	0.46	88.133	100
3	0.15	10.1	0.13	0.35	0.022	0.39	89.008	100
4	0.50	8.14	0.1	0.14	0.019	0.33	91.271	100
5	1.00	7.79	0.66	0.33	0.021	0.45	90.749	100
6	1.50	9.8	1.46	0.33	0.023	0.41	87.977	100
7	2.00	12	2.02	0.21	0.016	0.53	85.224	100
8	3.00	7.28	2.67	0.34	0.014	0.49	89.206	100
9	4.00	7.35	3.71	0.16	0.024	0.46	88.296	100
10	5.00	5.19	4.13	0.22	0.013	0.57	89.877	100
11	6.00	4.51	5.77	0.44	0.022	0.61	88.648	100
12	7.00	3.77	6.87	0.36	0.026	0.31	88.664	100

3.2.2 XRD Analysis

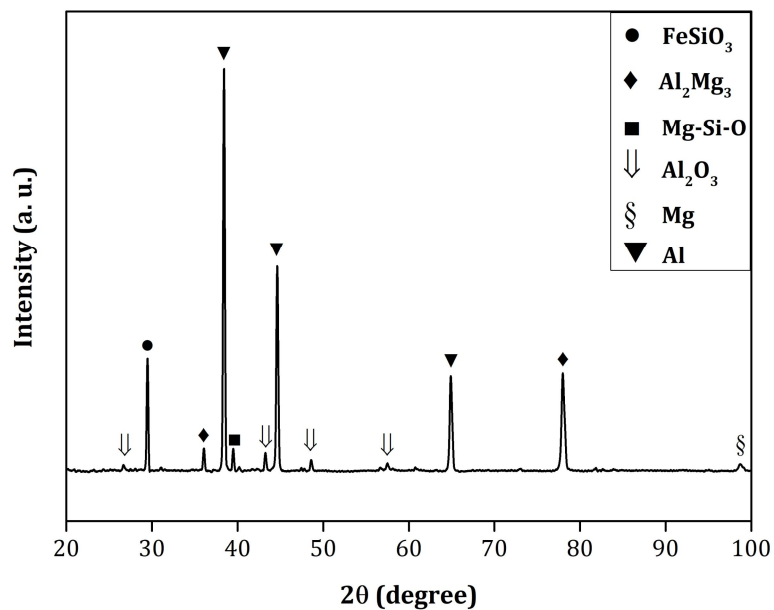


Figure 9 Typical XRD pattern of Al-Mg systems

3.2.3 Density and ductility

As shown in graph below, the density and ductility both reduced as magnesium concentration increased.

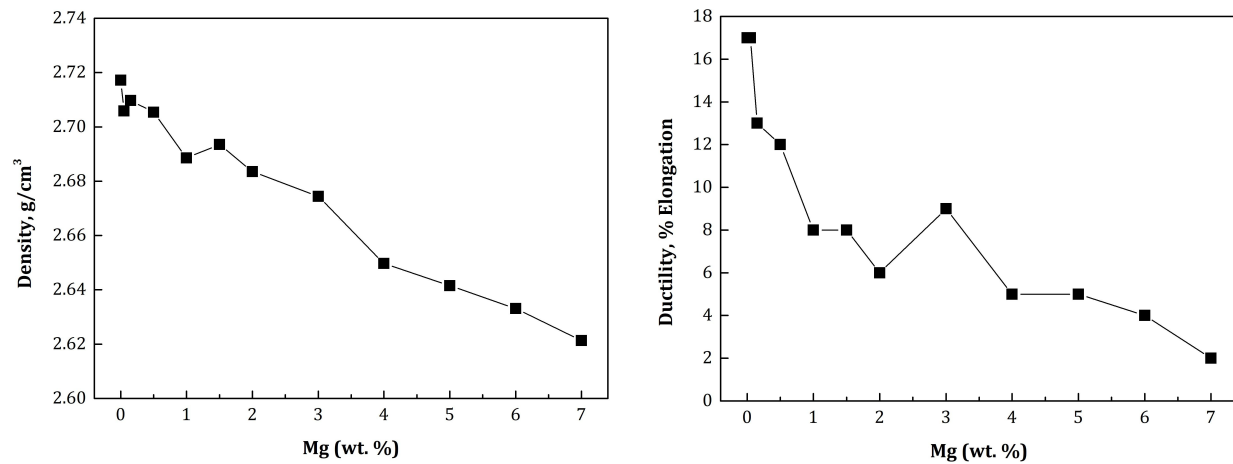


Figure 10 Variation of density and ductility in Al-Mg systems

3.2.4 Strength and hardness

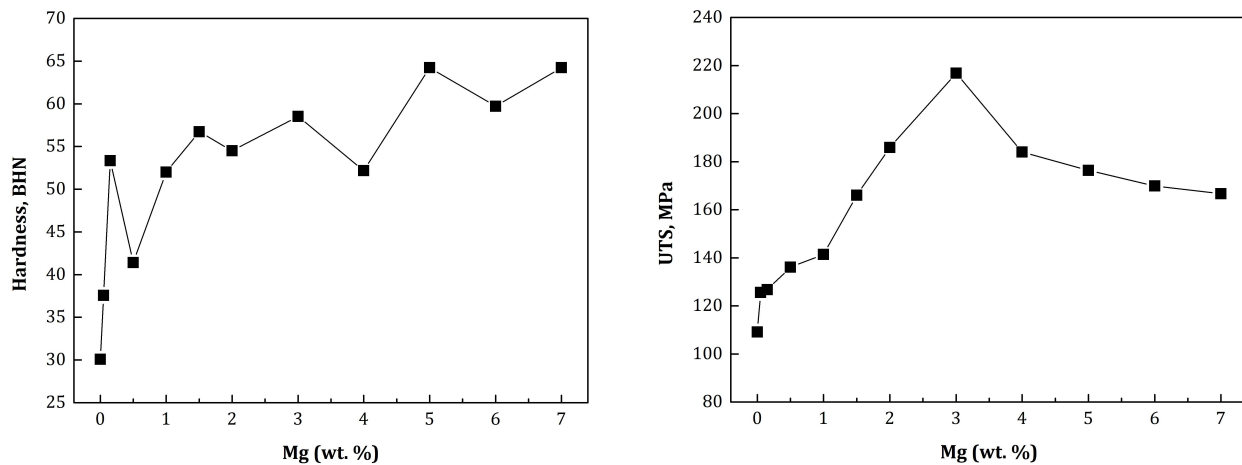


Figure 11 Variation of hardness and ultimate tensile strength in Al-Mg systems

As we can observe from the graphs above, the ultimate tensile strength was found increasing upto 3 wt % of magnesium concentration and then dropped. Hence specific strength, i.e., strength to density ratio also increases up to 3 wt % Mg and then decreased. After 4 wt % of magnesium, the slope of the graph became steady. Hardness increased throughout the addition of magnesium in the commercially pure aluminium.

3.2.5 Microstructure

Samples were prepared for microstructural analysis by standard metallographic technique without etching condition. Microstructural analyses by Optical Microscope and Scanning Electron Microscope (SEM) were performed as shown in following figure 12 and 13.

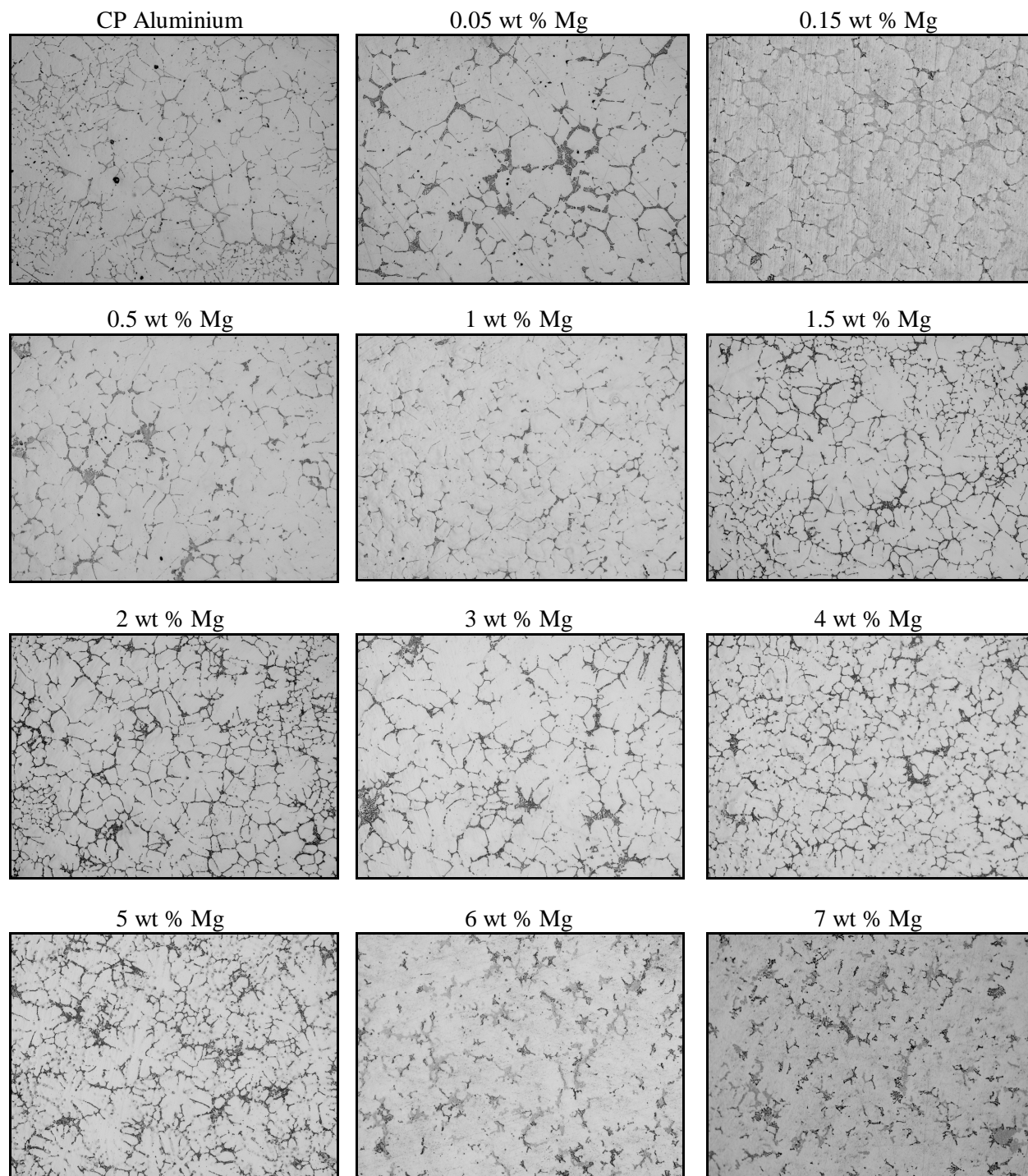
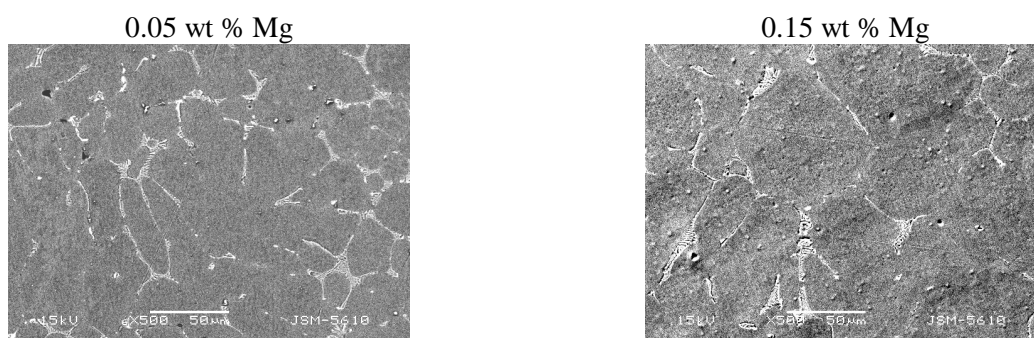


Figure 12 Optical Microstructure of Al-Mg systems at 100x magnification (Without Etching).



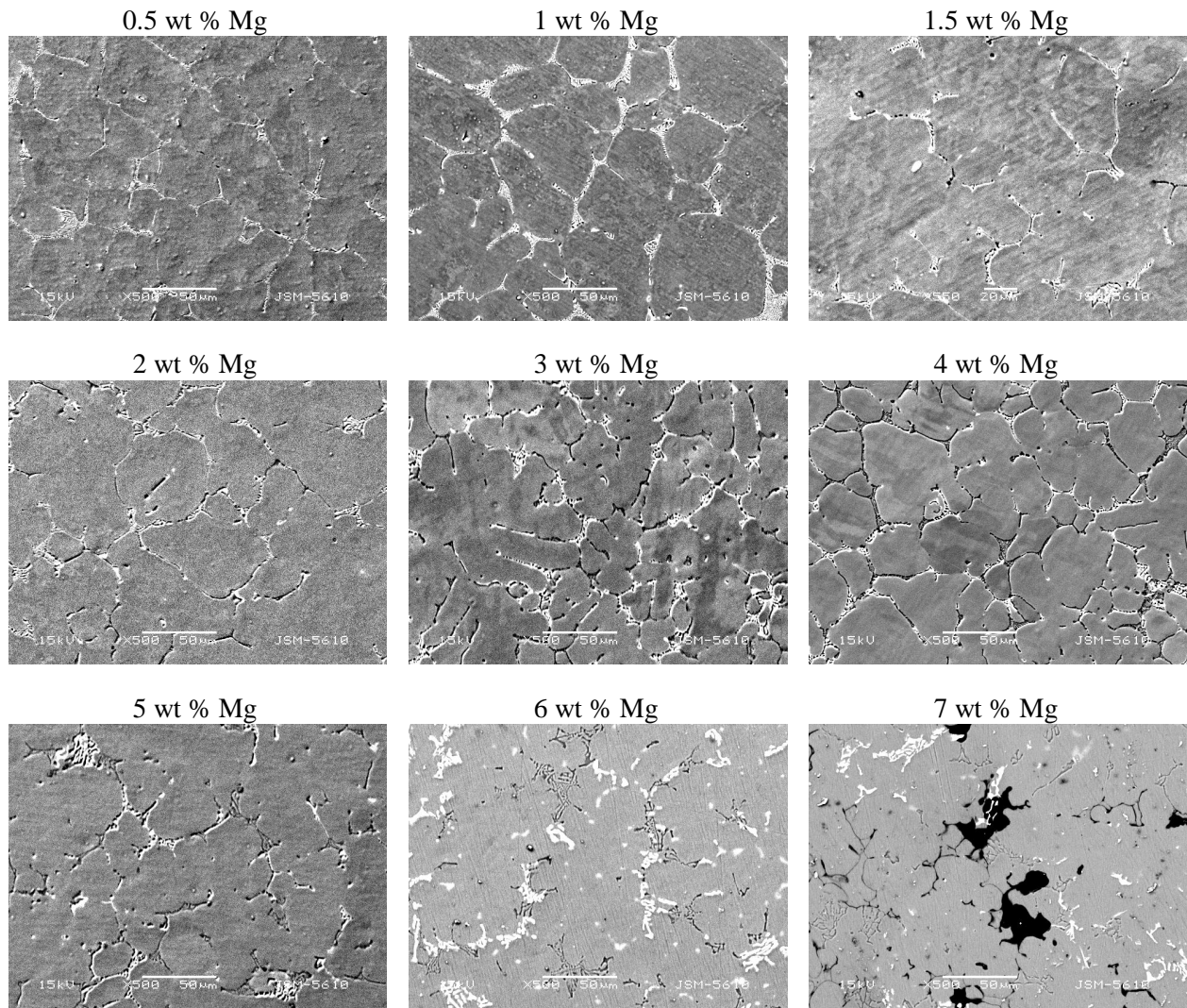


Figure 13 SEM Microstructure of Al-Mg systems at 500x magnification (Without Etching).

In these optical microstructures of various compositions, it was found that as the amount of Mg increased, the gathering and clustering of various intermetallics and unreacted (free form of) Mg at the grain boundary regions increased. This can be seen clearly from above optical micrographs where changes in morphology of grain boundary area were observed. These intermetallics are generally pushed towards the grain boundaries and accumulate there as solidification proceeds. This phenomenon of accumulation was nominal up to 3 wt % of Mg and became significant beyond 3 wt % of Mg. This resulted into variation of the shape, thickness and continuity of grain boundary regions, which can be confirmed in figure 12 and 13. Accumulation of unreacted Mg is also observed along with other intermetallic phases. It was because of the limited solubility of Mg with the Al beyond 3 wt % as per equilibrium phase diagram as is shown in figure 14.

The Al-Mg equilibrium phase diagram shows the variation in the solubility of Mg in Al with respect to temperature. The solubility of Mg decreases below 3 wt % in Al when temperature is reduced down to 100°C, whereas above 300°C all 7 wt % Mg can become soluble as is indicated by arrows in figure 14.

Maximum solubility of 17 to 18 wt % can be obtained as per equilibrium diagram at 450°C. In the present Al-Mg system, the amount of unreacted Mg available at room temperature increased as the concentration of Mg increased beyond 3 wt %. This unreacted Mg can act as a wetting site for ceramic particles during the formation of particulate reinforced metal matrix composites.

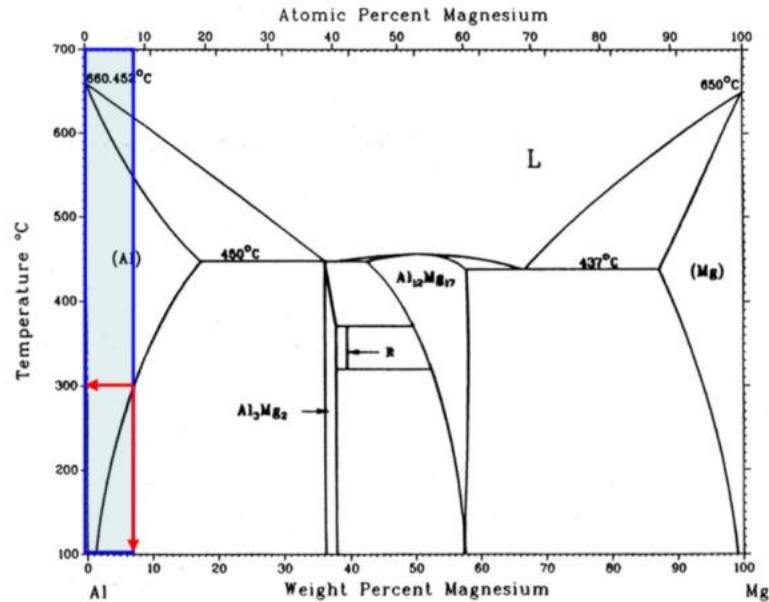


Figure 14 The equilibrium phase diagram of Al-Mg.

Characterization of the microstructures of the Al-Mg system in as cast condition revealed flawless grain structures. As shown in figures 12 and 13, the grain structure and various intermetallics like MgSiO_3 , Al_2O_3 , Mg-Si-O and Al_2O_3 etc., as light grey and white colour regions were observed. These have been confirmed by stoichiometric balance from EDS analysis for respective intermetallic phases. The microstructure analysis also revealed that columnar grains were absent and almost equiaxed grain structures were obtained. This is due to sufficient preheating of the metallic die before pouring, which reduces the thermal gradient during solidification.

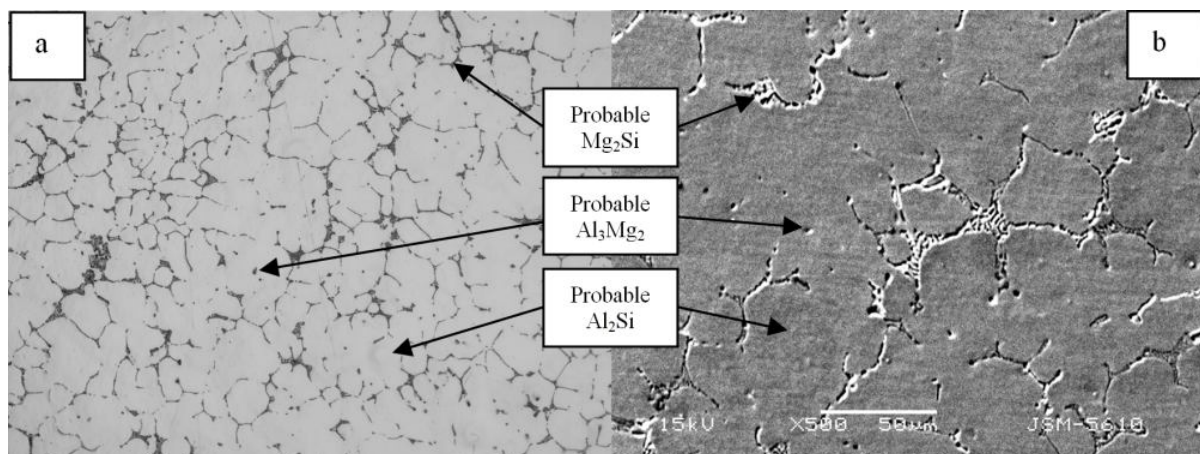


Figure 15 (a) Optical micrograph at 100x and (b) SEM micrograph at 500x, showing various probable intermetallic phases in Al-3 wt % Mg system.

3.3 Phase II: Effect of variation of MnO₂ by changing its addition sequence in CPA

3.3.1 Chemical analysis

Table 6 shows spectroscopy results of different experiments of Al-MnO₂ system.

Table 6 Chemical composition of Al-MnO₂ systems by spectroscopy (Element Recovery)

Experiments	Wt % MnO ₂ added	Element Composition (wt %)					
		<i>Si</i>	<i>Mn</i>	<i>Fe</i>	<i>O</i>	<i>Al</i>	<i>Total</i>
<i>Sequence A*</i>							
1	0.5	0.42	0.20	0.28	3.71	95.11	100
2	1.0	0.74	0.24	0.61	3.67	94.99	100
3	1.5	0.68	0.32	0.54	3.87	94.51	100
4	2.0	0.71	0.20	0.46	3.29	95.38	100
5	2.5	0.72	0.14	0.33	3.00	95.56	100
6	3.0	0.83	0.24	0.47	3.45	95.00	100
7	3.5	0.75	0.23	0.54	3.65	94.95	100
8	4.0	0.67	0.19	0.54	3.12	95.56	100
<i>Sequence B[#]</i>							
9	0.5	0.63	0.26	0.30	3.53	94.92	100
10	1.0	0.70	0.27	0.45	3.21	95.20	100
11	1.5	0.74	0.36	0.52	3.72	94.76	100
12	2.0	0.86	0.31	0.43	3.86	94.68	100
13	2.5	0.77	0.29	0.21	3.69	94.73	100
14	3.0	0.72	0.47	0.27	3.54	94.94	100
15	3.5	0.82	0.32	0.35	3.42	95.05	100
16	4.0	0.78	0.33	0.53	3.77	94.74	100

*Sequence A: MnO₂ added after melting of commercially pure aluminium and

[#]Sequence B: MnO₂ added before melting of commercially pure aluminium

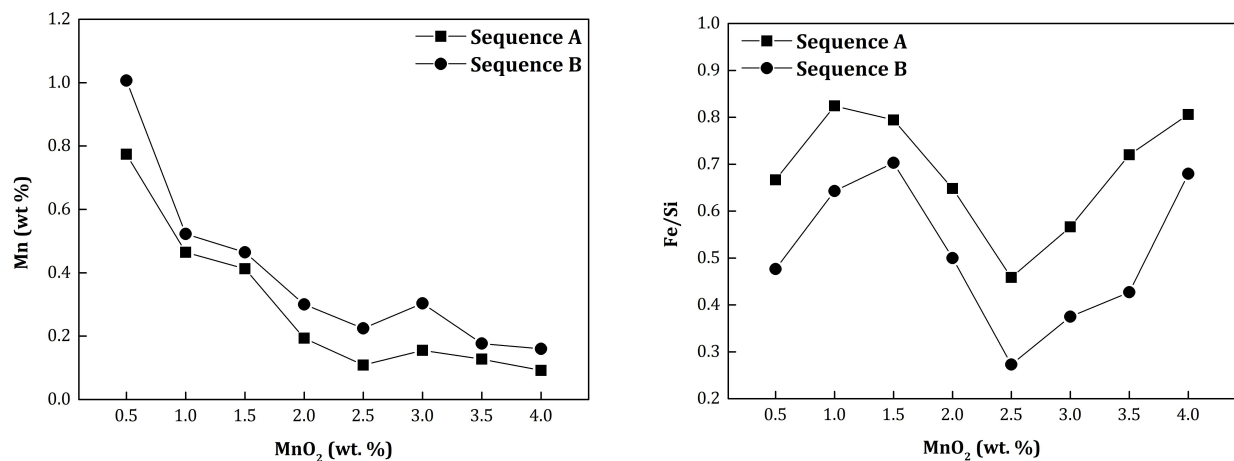


Figure 16 Manganese recovery and Fe/Si ratio in Al-MnO₂ systems.

3.3.2 X-Ray Diffraction

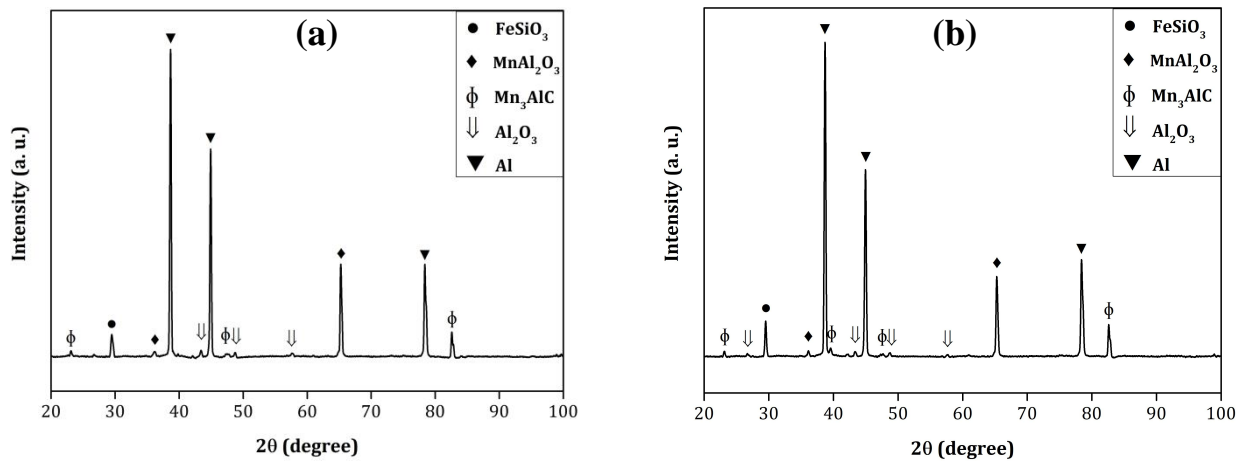


Figure 17 Typical XRD pattern of Al-2.5 wt % MnO₂ systems (a) sequence A and (b) sequence B.

Typical X-Ray pattern indicates the presence of complex carbides such as Mn₃AlC along with FeSiO₃, MnAl₂O₃ and Al₂O₃ into the aluminium matrix. Raw MnO₂ contained the carbon and hence in resultant in-situ composite produced complex carbides formation. No peak was observed of MnO₂ which indicated all MnO₂ has been consumed for the formation of various compounds.

3.3.3 Density and ductility

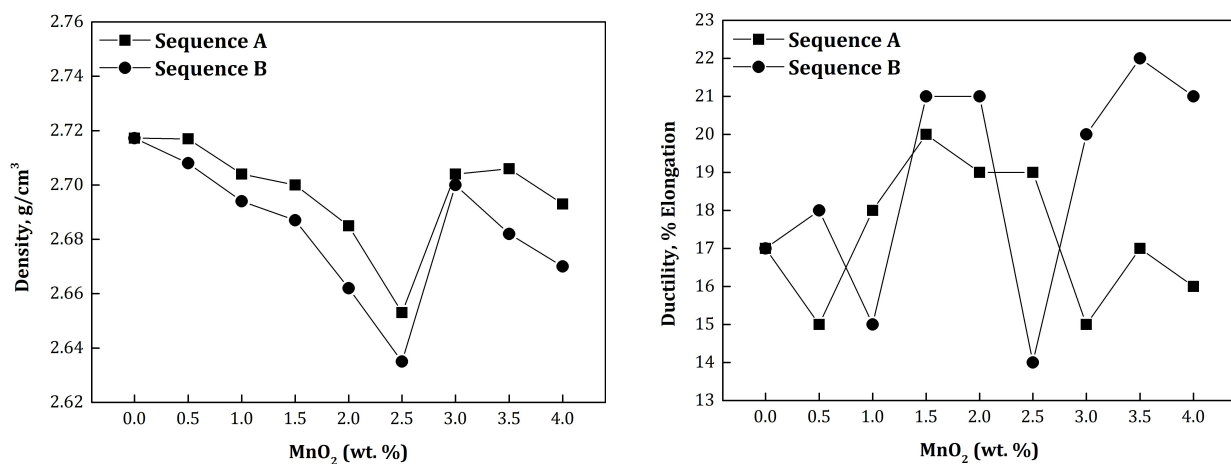


Figure 18 Variations of density and ductility in Al-MnO₂ systems.

As shown from figure 18, the density results were dropping from the initial value throughout the addition of MnO₂ in sequence A and B as per the trend line (curve fitting line). The ductility values were remained almost same and no marginal changes were observed in sequence A whereas it is increasing in sequence B as per the trend line as shown in the graphs, figure 18. The decreasing trend of density graphs indicates increasing in the amount of generated lighter phase. In this case carbides were generated and increased the hardness and strength compare to oxide.

3.3.4 Strength and hardness

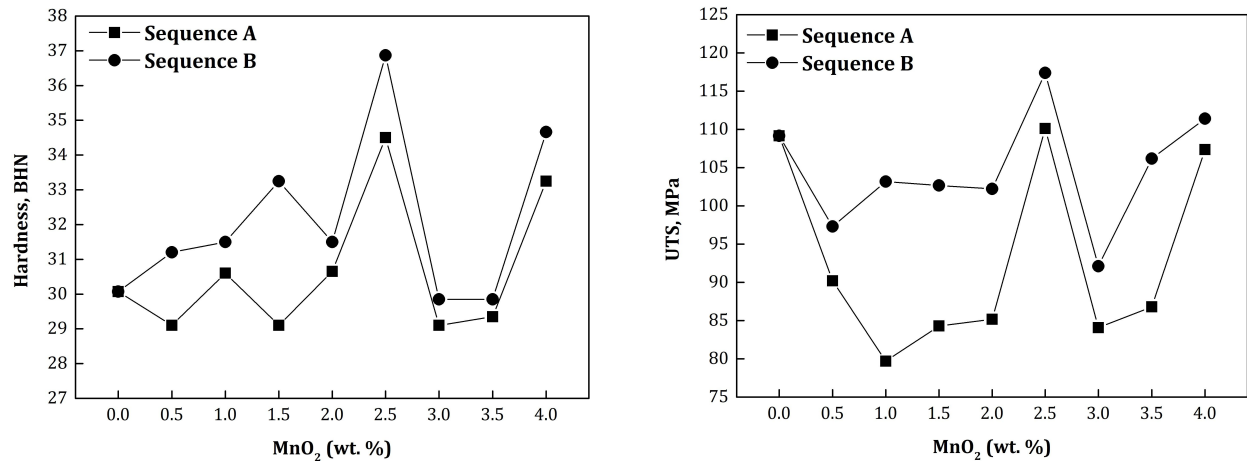
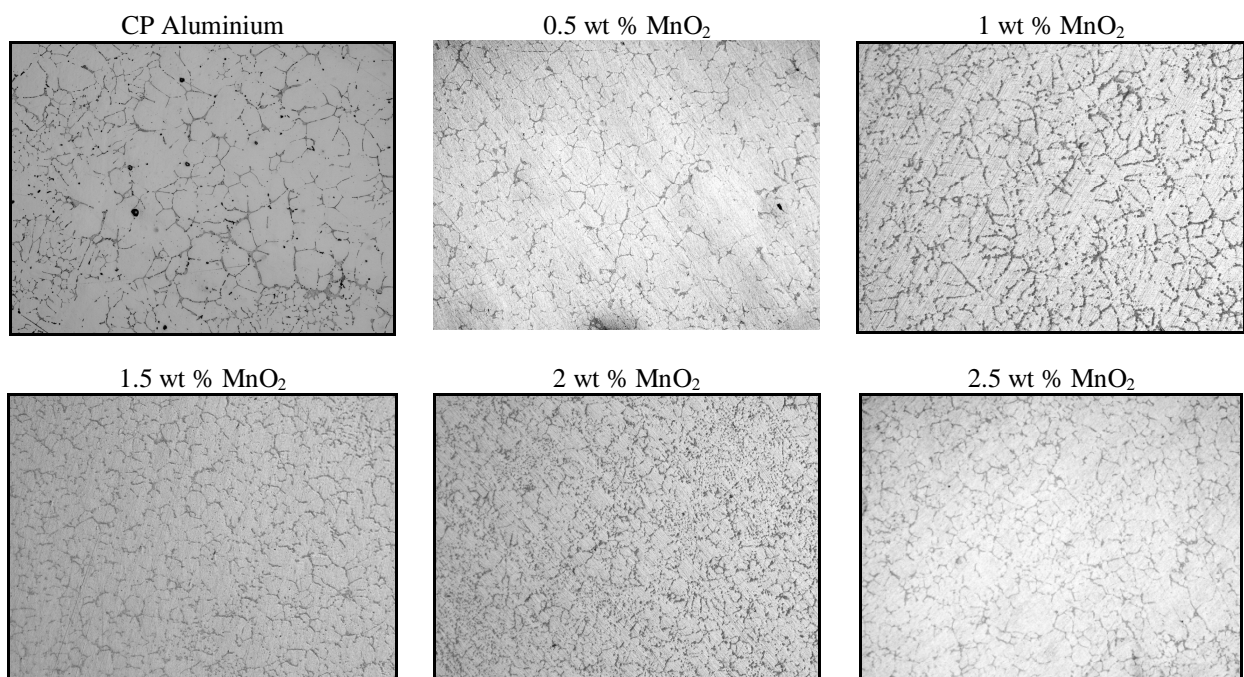


Figure 19 Variations of hardness and ultimate tensile strength in Al-MnO₂ systems.

As shown from figure 19, hardness distribution remains almost unchanged in entire system as per the trend line in sequence A. But in sequence B, hardness value increases as amount of MnO₂ added. Similarly as indicated in figure 19, the slight reduction in ultimate tensile strength values were observed in sequence A while in sequence B, it increases as MnO₂ increases. Although the highest hardness values were observed in 2.5 wt % MnO₂ combination in the both sequences A and B whereas the highest UTS was found in sequence A at 2.5 wt % MnO₂ compositions and at 2 wt % MnO₂ in sequence B.

3.3.5 Microstructure

Sequence A



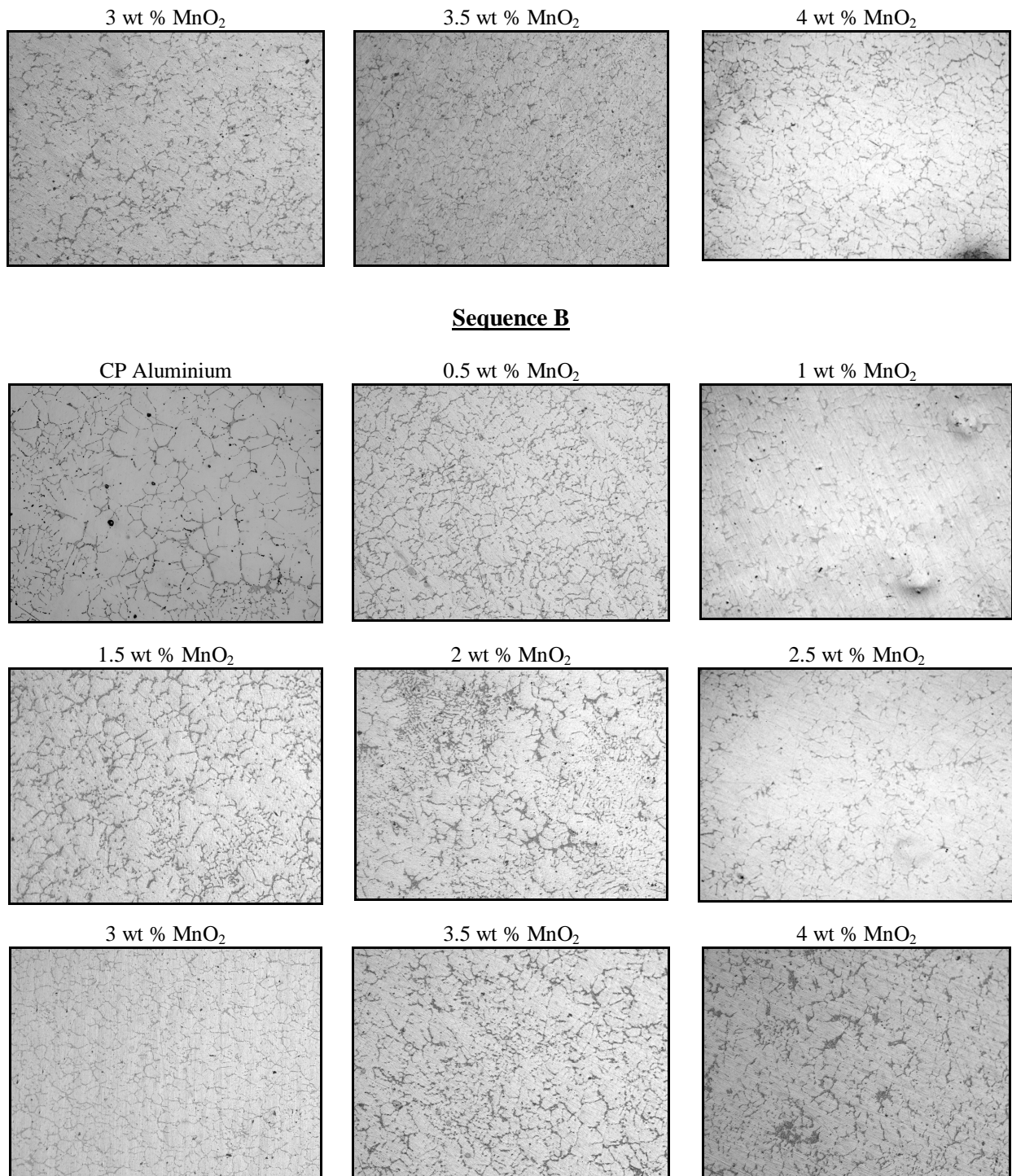


Figure 20 Optical Microstructure of Al-MnO₂ systems at 100x magnification (Without Etching)

Both optical and SEM microstructures shown in above figure 20, 21 and 22 consist of results of both the sequence A and B. Compare to sequence A, sequence B microstructures show more uniformity as far as morphology of grain boundaries and other resultant phases are concerned. As we can compare both micro results, the addition of MnO₂ as in sequence A gave more bulky grain boundaries and segregated phases whereas in sequence B thin grain boundaries are observed. Also resultant phases were found well distributed in sequence B. The microstructures were having no porosity.

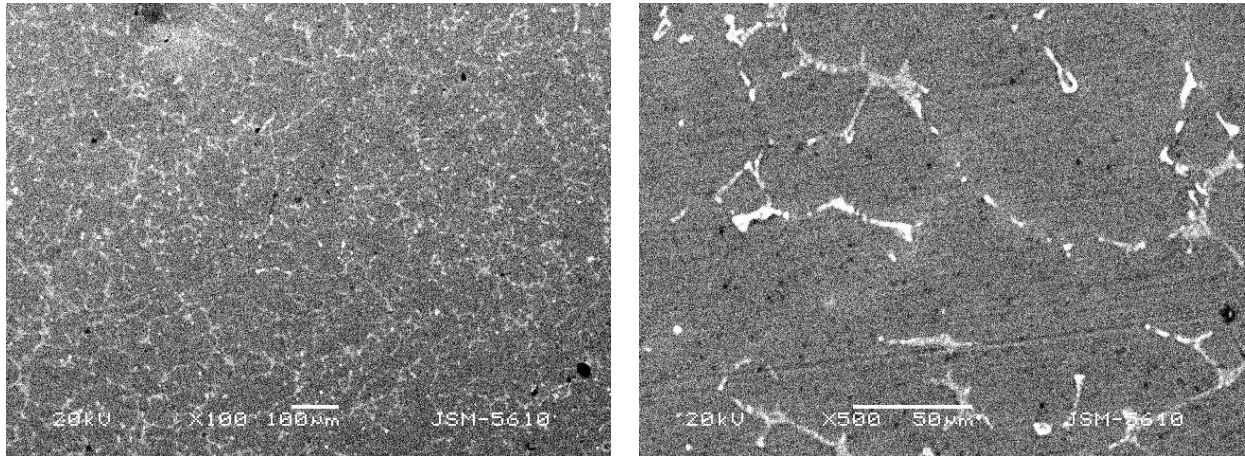


Figure 21 SEM images of 2.5 wt % MnO_2 in sequence A at (a) 100x and (b) 500x magnification (Without Etching).

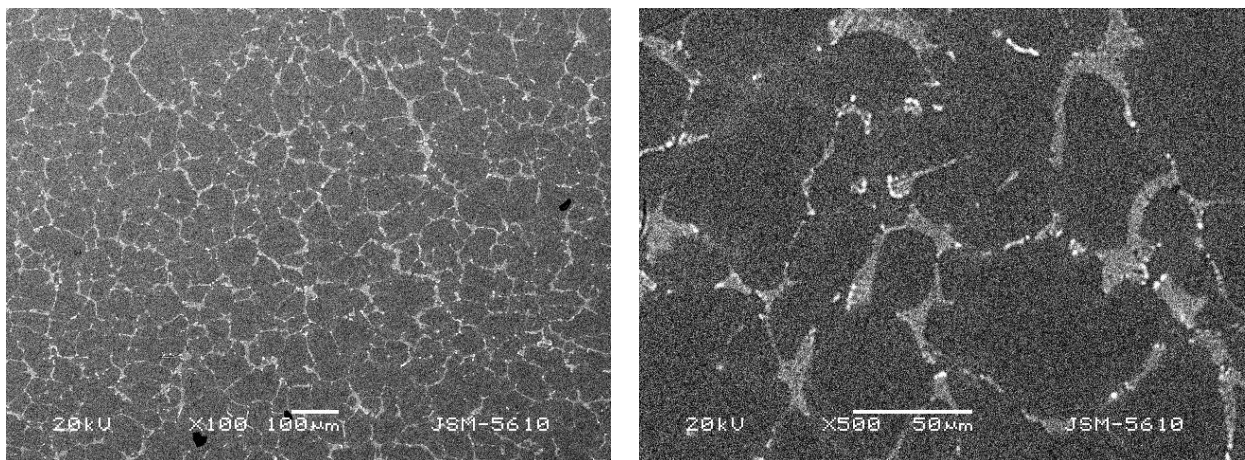


Figure 22 SEM images of 2.5 wt % MnO_2 in sequence B at (a) 100x and (b) 500x magnification (Without Etching).

3.4 Phase III: Effect of variation of MnO_2 by changing its addition sequence in CPA along with optimized magnesium metal from phase I study

3.4.1 Chemical analysis

Table 7 shows spectroscopy results of different experiments of Al-Mg system.

Table 7 Chemical compositions of various Al- MnO_2 systems by spectroscopy (Element Recovery).

Experiments	Wt % Mg added	Wt % MnO_2 added	Element Composition (wt %)					Total
			Mg	Si	Mn	Fe	Al	
<i>Sequence A*</i>								
1	3	1.0	2.61	0.73	0.25	0.79	94.43	100
2	3	2.5	2.43	0.58	0.66	0.74	95.97	100
3	3	4.0	2.38	0.72	0.92	0.63	93.84	100
<i>Sequence B[#]</i>								
4	3	1.0	2.67	1.43	0.31	1.16	95.69	100
5	3	2.5	2.68	2.57	0.93	0.95	95.54	100
6	3	4.0	2.71	3.56	1.08	1.62	91.79	100

*Sequence A: MnO_2 added after melting of commercially pure aluminium (conventional route) and

[#]Sequence B: MnO_2 added before melting of commercially pure aluminium (non-conventional route)

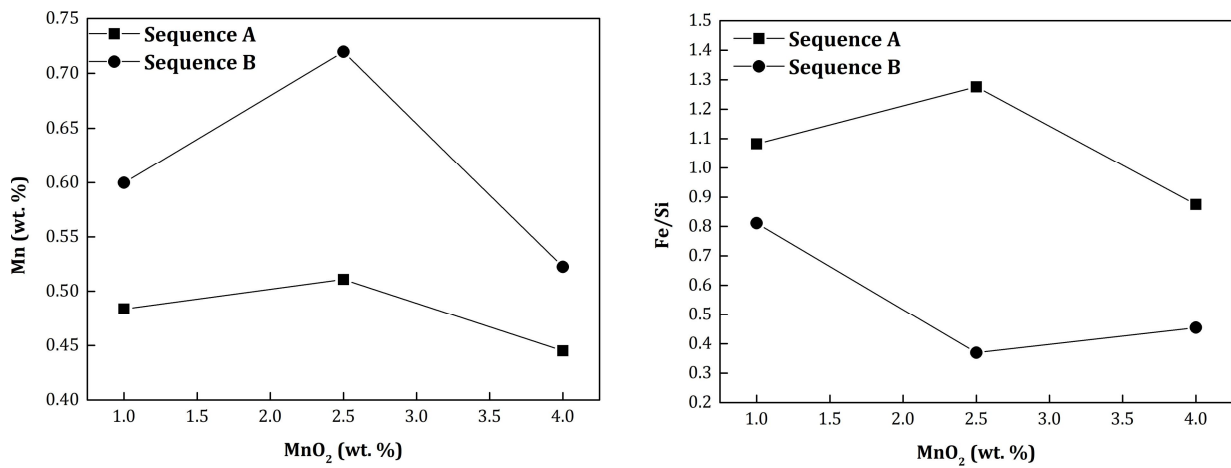
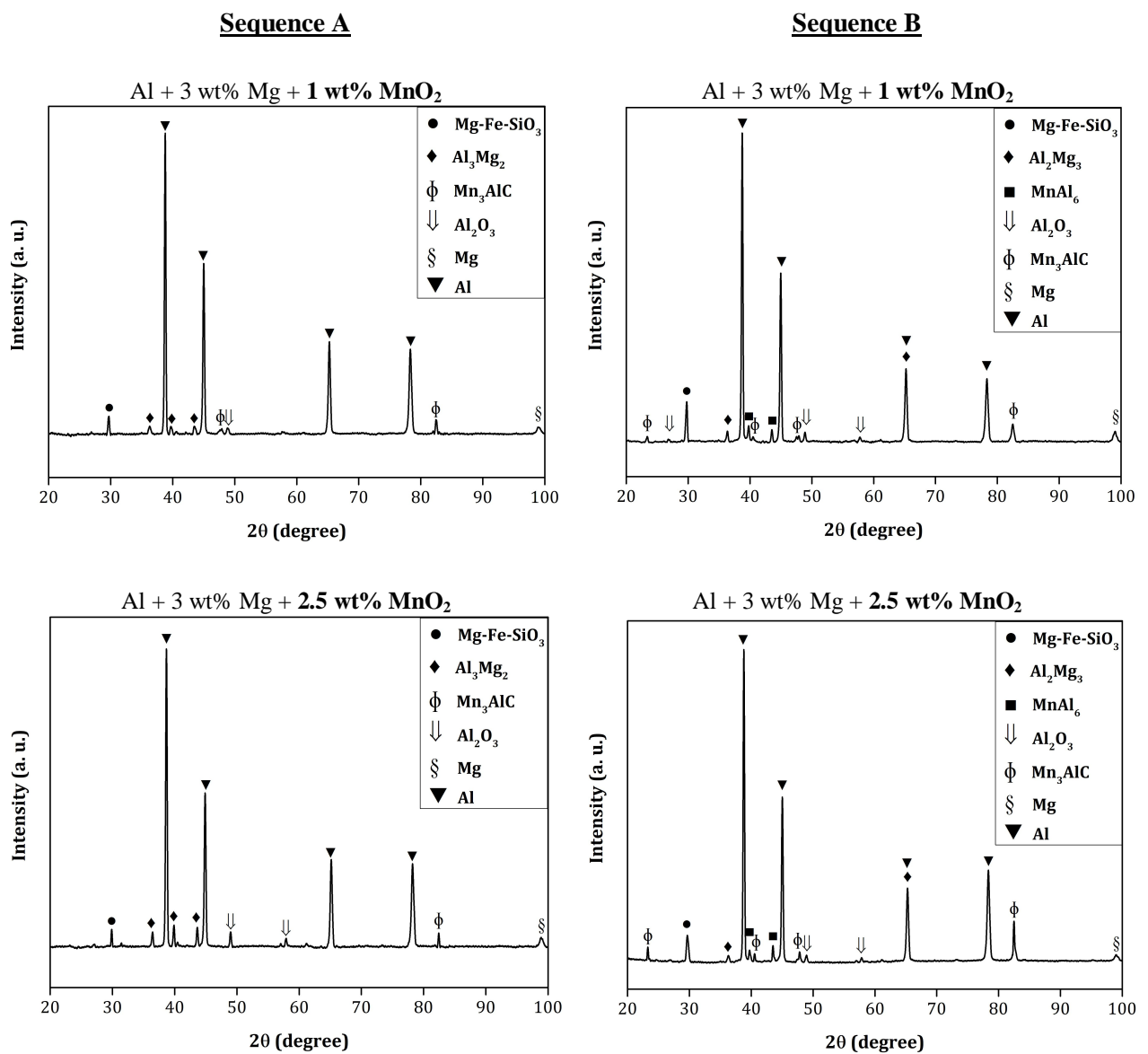


Figure 23 Manganese recovery and Fe/Si ratio in Al-3 wt % Mg-MnO₂.

3.4.2 X-Ray Diffraction



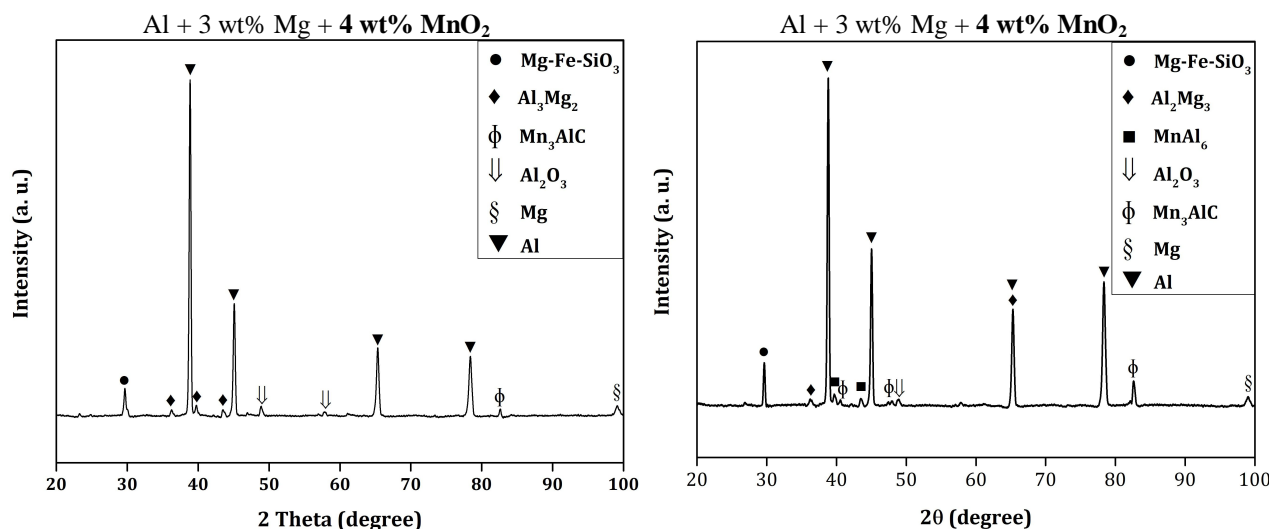


Figure 24 Typical X-ray diffraction patterns of various Al-3 wt % Mg-MnO₂ systems.

All X-Ray patterns show almost similar patterns and compounds peaks. The presence of the in-situ complex carbide compounds such as Mn₃AlC along with Mg-Fe-SiO₃, Al₃Mg₂, Al₂Mg₃, Al₂O₃ and Mg were confirmed in below XRD patterns. It was noted that the peak height of Mn₃AlC in 2.5 wt % MnO₂ in sequence B experiments are higher as compared to all the combinations of sequence A experiments. This could be the main reason to have improved mechanical properties in this system following sequence B.

3.4.3 Density and ductility

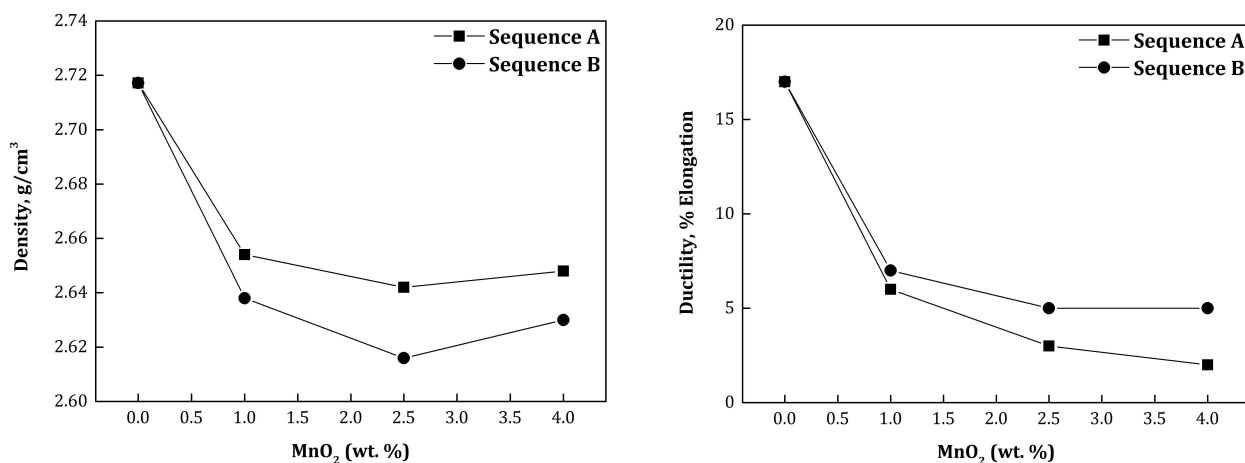


Figure 25 Variation of density and ductility of Al-3 wt % Mg-MnO₂ systems with respect to MnO₂ content.

Density of the Al-Mg-MnO₂ system decreased throughout the experiments as compared to the base material whereas same trend can be observed in ductility, in terms of % elongations too. Formation of the lighter phases is responsible for dropping both ductility as well as density as indicated in XRD patterns.

Lowest density was observed at Al-Mg-1 wt % MnO₂ system after which it increased little bit in both sequences A and B. Similarly the ductility lowest value was obtained in Al-Mg-2.5 wt % MnO₂ system and then improved. Overall both ductility and density were marginally lowered in both sequences as compared to the base material value.

3.4.4 Strength and hardness

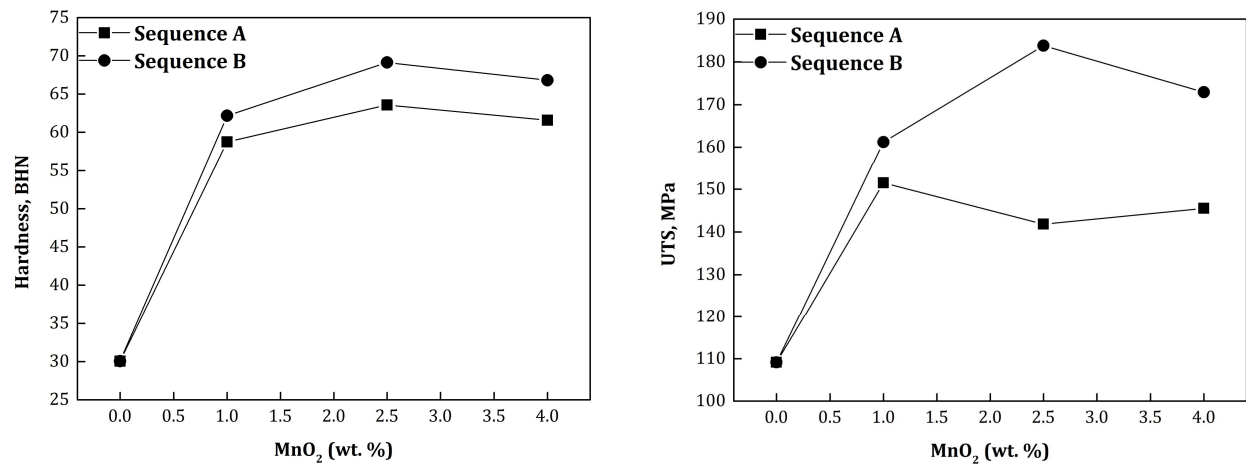


Figure 26 Effect of MnO₂ additions on hardness and ultimate tensile strength in Al-3 wt % Mg-MnO₂ systems.

Ultimate tensile strength (UTS) was found improved in both sequences as compared to base material. Trend of UTS is found more increasing in sequence B as compared to sequence A. Highest value of UTS was found in Al-Mg-4wt % MnO₂ in sequence B.

3.4.5 Microstructure

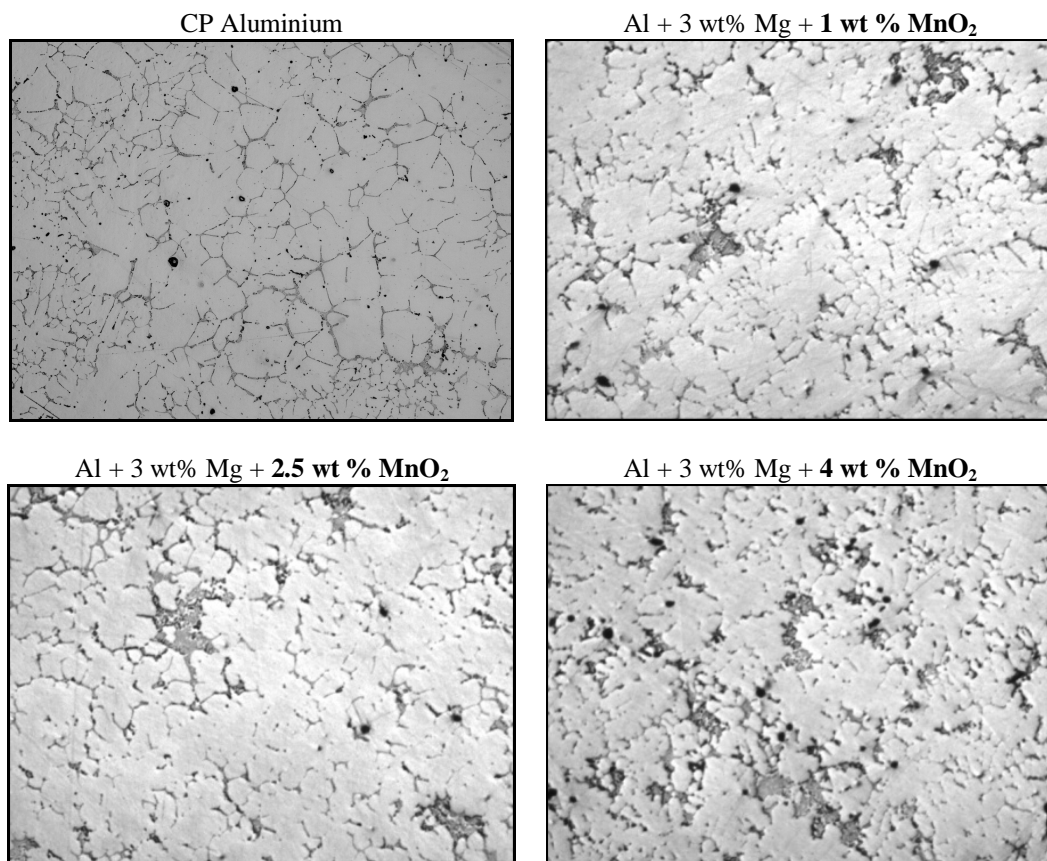


Figure 27 Optical microstructures of various Al-3 wt % Mg-MnO₂ systems at 100x in sequence A (Without Etching).

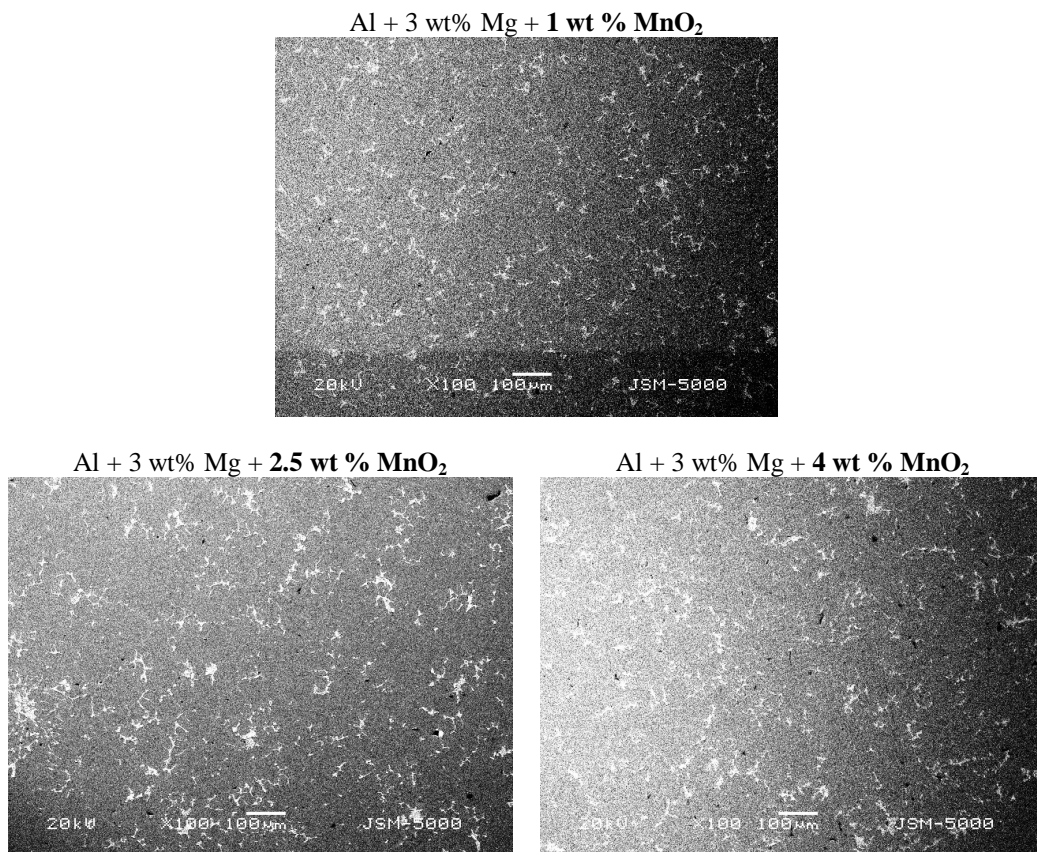


Figure 28 SEM images of different Al-3 wt % Mg-MnO₂ systems at 100x in sequence A (Without Etching).

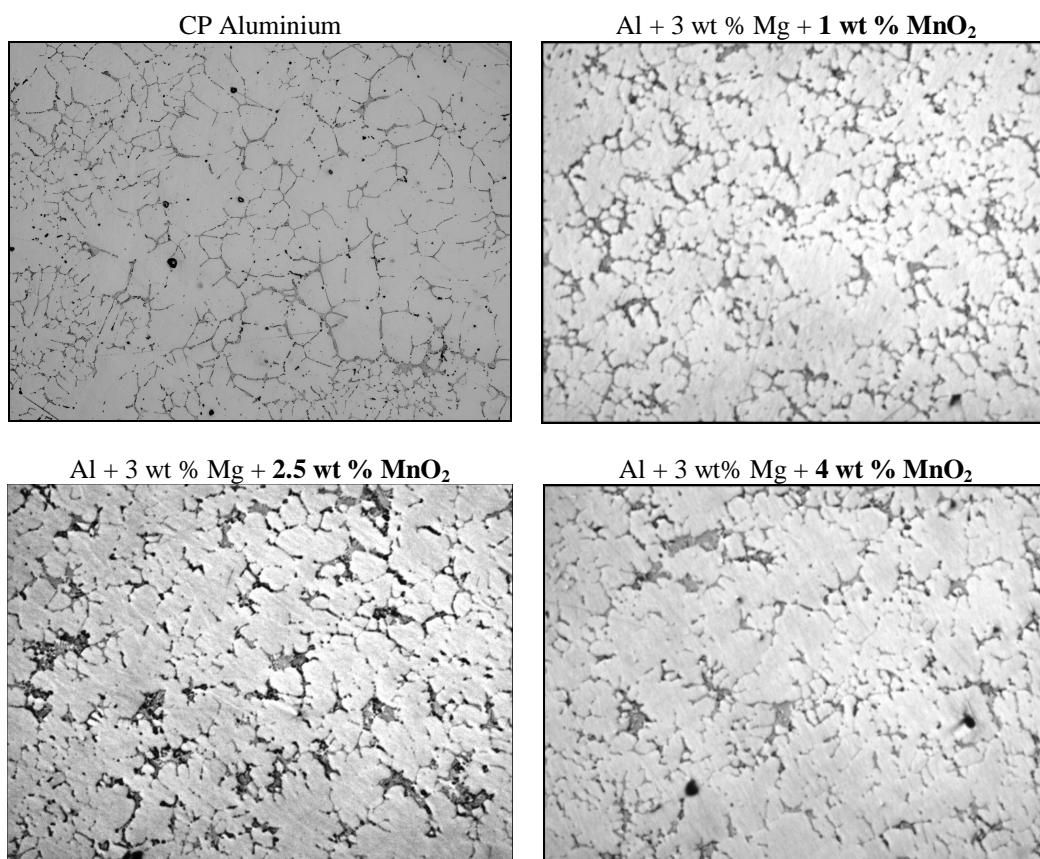


Figure 29 Optical microstructures of different Al-3 wt % Mg-MnO₂ systems at 100x in sequence B (Without Etching).

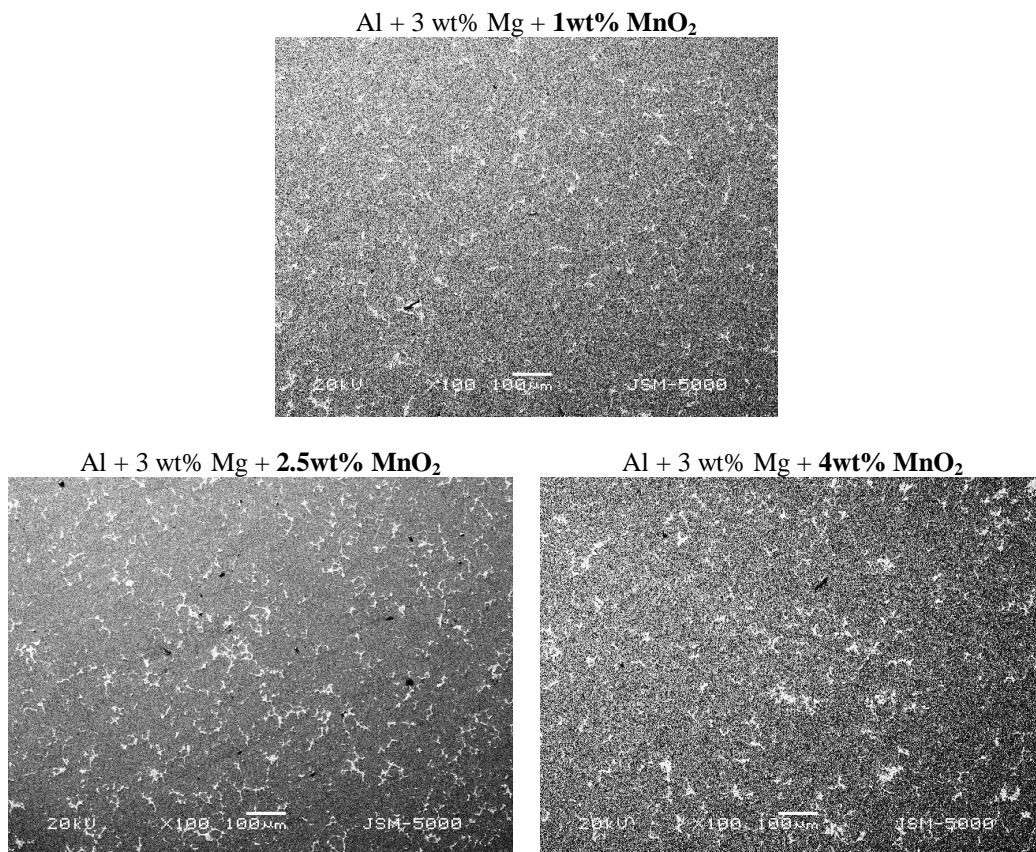


Figure 30 SEM images of different Al-3 wt % Mg-MnO₂ systems at 100x in sequence B (Without Etching).

Optical microstructures of Al-3 wt% Mg-MnO₂ system were prepared by standard metallographic practice without etching as shown in figures 27 (sequence A) and figure 29 (sequence B). SEM micrographs of sequence A and B are shown in figure 28 and 30 respectively. In the microstructure, highest refinement was observed in Al-3 wt% Mg-1 wt% MnO₂ system in sequence B as shown in figures. It also confirmed from SEM micrographs. More phase formation appeared in Al-3 wt% Mg-1 wt% MnO₂. Also the distribution of Al-Mn complex carbide was found uniform.

4. CONCLUSION

From above research work, following conclusions can be drawn for different phase of experiments.

For Phase I:

- a. Both, density and ductility results were decreased in the Al-Mg system throughout the variation of magnesium content. Since the density of magnesium is lower than the aluminium, it made the overall system lighter. However, due to some brittle phases and its stress raising effect, the ductility of the system dropped.
- b. The hardness results (BHN) of Al-Mg system were found increasing continuously as magnesium concentration increased because of formation and accumulation of the phases such as MgSiO₃ and Al₂Mg₃ at the grain boundaries while synthesis.

- c. Ultimate tensile strength was found maximum at 3 wt % Mg. For higher magnesium concentrations, due to limited solubility of magnesium in aluminium, unreacted magnesium formed which was accumulated at the grain boundaries. This results in weakening of the grain boundaries.
- d. The generated phases were found uniformly distributed at grain boundaries in the microstructures up to 3 wt % Mg. Unreacted magnesium along with other phases were present after 3 wt % Mg, which adversely affected various properties of Al-Mg system.
- e. Al-3 wt % Mg system was found to be optimum because of the good combination of various properties like microstructure, ultimate tensile strength, specific strength and hardness with low density. Hence, Al-3 wt % Mg system is quite good for manufacturing of the low cost Al-Mg alloy with highest possible metallurgical and mechanical properties.

For Phase II:

- a. The Al-MnO₂ composite systems were synthesised by stir casting method. The different amount of MnO₂ powder was added into the commercially pure aluminium in two different sequences A and B. In sequence B, when MnO₂ powder was added into solid commercially pure aluminium in the beginning of the experiments (before melting of commercially pure aluminium), due to sufficient time involved in decomposition of MnO₂, various favourable chemical reactions were possible. Hence in sequence B, metallurgically sound structure was obtained which is giving highest value of hardness and ultimate tensile strength in Al-2.5 wt % MnO₂ system.
- b. The MnO₂ particles were decomposed and formed in-situ phases and complex carbide of Al and Mn. Various in-situ generated phases into the final composite materials which were confirmed by the XRD analysis are FeSiO₃, MnAl₂O₃, Al₂O₃ and Mn₃AlC.
- c. It is observed that the ductility, hardness and ultimate tensile strength results were increased when MnO₂ particles were added into commercially pure aluminium before its melting (Sequence B) compared to the results when MnO₂ particles were added into commercially pure aluminium after its melting (Sequence A). Hence sequence B is more promising as far as metallurgical and mechanical properties are concerned.

For Phase III:

- a. In this analysis, the optimization of MnO₂ was studied using the commercially pure aluminium and optimized 3 wt % magnesium (from phase I study) matrix system. The amount of MnO₂ particles and the sequence of its addition were changed like in phase II analysis. The results of both, density and ductility were decreased whereas the hardness values were increased in present Al-3 wt % Mg-MnO₂ system in both A and B sequences. The results of tensile strength in sequence B were observed marginally improved compared to sequence A experiments.
- b. Various in-situ phases and complex carbides were generated in present Al-3 wt % Mg-MnO₂ system such as MgFeSiO₃, Al₃Mg₂, Mn₃AlC and Al₂O₃ in sequence A whereas MgFeSiO₃, Al₂Mg₃, Mn₃AlC, MnAl₆ and Al₂O₃ in sequence B analysis. The distribution of these in-situ

generated phases were found maximum in Al-3 wt % Mg-2.5 wt % MnO₂ system of sequence B experiments as observed from microstructures.

- c. Microstructures of Al-3 wt % Mg-MnO₂ in-situ composites showed effective dispersion of various above mentioned in-situ generated phases and compounds. Analysis of some regions was confirmed the recoveries of manganese which were higher in sequence B experiments as compared to sequence A experiments. Such in-situ phases were found accumulated at the grain boundaries while grain growth.

OVERALL Conclusions:

The following final conclusions can be made from all above phases are:

- a. *In phase I study*, Al-3 wt % Mg system giving highest values of mechanical properties for present commercially pure Al metal.
- b. *In phase II study*, the sequence B for MnO₂ addition is found more promising, i.e. when MnO₂ added in commercially pure aluminium before its melting as far as mechanical properties are concerned. The result trend lines in graphs are steeper in sequence B compared to sequence A. In sequence B, the microstructures are much more refined and average value of Mn recovery is improved.
- c. *In phase III study*, magnesium amount was kept fixed 3 wt % as optimized in phase I, the best sequence of addition of MnO₂ was sequence B i.e. MnO₂ addition in commercially pure aluminium before its melting because the micromechanical results are more favourable than sequence A. Average recovered Mg and Mn both are higher in sequence B as compared to A. It promotes the formation various in-situ phases as indicated in XRD analysis which strengthen the matrix.

Using above approach, the manufacturing of light weight Aluminium Metal Matrix Composites (AMMCs) can be promoted to achieve good micromechanical properties at lower cost as compared to the conventional materials and method of manufacturing.

REFERENCES

1. Zaid B. Jildeh, et. al., "Thermocatalytic behavior of Manganese (IV) Oxide as Nanoporous Material on the Dissociation of a Gas Mixture Containing Hydrogen Peroxide", *Nanomaterials* 2018, 8, 262
2. J. Zhang, Z. Fan, Y.Q. Wang and B.L. Zhou, "Microstructural evolution of the in situ Al-15wt.%Mg₂Si composite with extra Si contents", *Scripta mater.* 42 (2000) 1101–1106
3. Rub Nawaz Shahid and Sergio Scudino, "Microstructure and Mechanical Behavior of Al-Mg Composites Synthesized by Reactive Sintering", *Metals* 2018, 8, 762
4. Ashis Mallick, "Improvement of mechanical properties in light weight Mg-based materials", *Procedia Engineering* 149 (2016) 283 – 287

5. H. N. Panchal and V. J. Rao, "Influence of Mg on micro-mechanical behaviour of as cast Al-Mg System", *Physics of Metals and Metallography*, 2019, Vol. 120, No. 9, pp. 881–887.
6. H. N. Panchal and V. J. Rao, "Preparation of Al-MnO₂ Composite using Stir Casting Method", *Proceedings of International Conference on Recent Advances in Metallurgy for Sustainable Development (IC-RAMSD 2018)*, ISBN : 978-93-88879-64-4, February 1st-3rd, 2018, The M. S. University of Baroda, Vadodara, India.
7. Abdulhaqq A. Hamid, P. K. Ghosh & Subrata Ray, "Processing, Microstructure & Mechanical Properties of Cast In-Situ Al(Mg, Mn)-Al₂O₃(MnO₂) Composite", A post-doctoral research paper, *Met. & Matr. Trans A*, 2005, 36A, pp: 2211 - 2223.
8. Abdulhaqq A. Hamid, P. K. Ghosh & Subrata Ray, "Characterization & Tribological behavior of cast In-Situ Al(Mg, Mo)-Al₂O₃(MoO₃) Composite", A post-doctoral research paper, *Met. & Matr. Trans B*, 2006, 37B, pp: 519-529.
9. Abdulhaqq A. Hamid, P. K. Ghosh & Subrata Ray, "Processing, Microstructure & Mechanical Properties of Cast In-Situ Al(Mg, Ti)-Al₂O₃(TiO₂) Composite", A post-doctoral research paper, *Metal Trans A*, 2006, 37A, pp: 469 – 480.
10. A Olszówka-Myalska and W Maziarz, "Microstructural analysis of titanium aluminide formed in situ in an aluminium matrix composite", *IOP Conf. Series: Materials Science and Engineering 7* (2010) 012021
11. H. X. Peng, D. Z. Wang, L. Geng and C. K. Yao, "Evaluation of The Microstructure of In-situ Reaction Processed Al₃Ti-Al₂O₃-Al Composite", *Scripta Mat.* Vol. 37, No. 2, pp. 199-204, 1997
12. M. Dyzia, J. Oeleziona, "Aluminium matrix composites reinforced with AlN particles formed by in situ reaction", *Archives of Materials Science and Engineering*, Volume 31, Issue 1, May 2008, pp: 17-20
13. H. X. Peng and Z. Fan, "In situ Al₃Ti-Al₂O₃ intermetallic matrix composite: Synthesis, microstructure, and compressive behavior", *J. Mater. Res.*, Vol. 15, No. 9, Sep 2000, pp: 1943-1949.
14. Q. Zhang, B.L. Xiao, W.G. Wang, Z.Y. Ma, "Reactive mechanism and mechanical properties of in situ composites fabricated from an Al-TiO₂ system by friction stir processing", *Acta Materialia* 60 (2012), pp: 7090–7103
15. Metin Onal and Mehmet Gavgali, "Production of Metal Matrix Composites by In situ Techniques", *Journal of Scientific and Engineering Research*, 2017, 4(2):78-82
16. Biswajit Das, Susmita Roy, Ram Naresh Rai and S.C. Saha, "Development of an in-situ synthesized multi-component reinforced Al-4.5%Cu-TiC metal matrix composite by FAS technique – Optimization of process parameters", *Engineering Science and Technology, an International Journal* (2015)
17. Zhang Xiuqing, Liao Lihua, Ma Naiheng, Wang Haowei, "New In-situ Synthesis Method of Magnesium Matrix Composites Reinforced with TiC Particulates", *Materials Research*, Vol. 9, No. 4, 357-360, 2006
18. Mahmoud M. Tash and Essam R. I. Mahmoud, "Development of in-Situ Al-Si/CuAl₂ Metal Matrix Composites: Microstructure, Hardness, and Wear Behavior", *Materials* 2016, 9, 442; doi:10.3390/ma9060442

19. Lawrance C. A. and Dr. P. Suresh Prabhu, “Stir Casting of in-situ Al 6061TiB₂ Metal Matrix Composite Synthesized with Different Reaction Holding Times”, International Journal of Engineering Research & Technology (IJERT), Vol. 4 Issue 09, September-2015
20. E. Georgatis, A. Lekatou, A.E. Karantzalis, H. Petropoulos, S. Katsamakis and A. Poulia, “Development of a Cast Al-Mg₂Si-Si In Situ Composite: Microstructure, Heat Treatment, and Mechanical Properties”, Journal of Materials Engineering and Performance Volume 22(3) March 2013, 729-741
21. Vikas Narain and Subrata Ray, “Comparative study of mechanical properties of cast and forged Al-3Mg-MnO₂ and Al-8Mg-MnO₂ composites”, Heliyon 6 (2020) e03275
22. Vikas Narain and Subrata Ray, “Variation in mechanical properties with MnO₂ content in cast and forged in-situ Al-8Mg-MnO₂ composites”, j mater res technol. 2019; 8(5):4489–4497
23. C. S. Ramesh, S. Pramod, R. Keshavamurthy, “A study on microstructure and mechanical properties of Al 6061–TiB₂ in-situ composites”, Materials Science and Engineering A 528 (2011) 4125–4132
24. S. L. Pramod, Srinivasa R. Bakshi, and B. S. Murty, “Aluminum-Based Cast In Situ Composites: A Review”, Journal of Materials Engineering and Performance, 2015